

Delay-Constrained Random Access Transport Capacity

Ilmu Byun, *Student Member, IEEE*, Jeffrey G. Andrews, *Fellow, IEEE*,
and Kwang Soon Kim, *Senior Member, IEEE*

Abstract—In this paper, we consider delay-constrained wireless multi-hop ad hoc networks where a packet should be delivered to the destination within the maximum allowed delay while satisfying the target outage probability. The proposed performance metric for analyzing networks is the delay-constrained random access transport capacity (D-RATC), which quantifies the maximum end-to-end (e2e) link achievable rate per unit area of a delay-constrained network using a random access protocol. The scaling of the D-RATC is obtained for various slotted ALOHA (SA) protocols and it is shown that the SA protocol is order-optimal for delay-constrained random networks when interference control is used with an additional feature such as rate control or admission control. If interference control is not used, the SA protocol suffers from the negatively infinite scaling exponent except the case of using rate control where a finite but suboptimal scaling exponent may be achieved. Also, it is shown that multi-hop control does not affect the scaling exponent but just improves the D-RATC pre-constant.

Index Terms—Ad hoc networks, random access transport capacity, capacity scaling, delay-constrained capacity.

I. INTRODUCTION

A WIRELESS ad hoc network is an uncoordinated network in which nodes communicate without centralized control or wired infrastructure. The performance of an ad hoc network has been typically analyzed in terms of the capacity scaling [1]–[11] which denotes the order of the growth of a scalar performance metric as the number of source nodes in the network increases. In [1], the optimal capacity scaling of an arbitrary static network was shown to be $\Theta(\sqrt{n})$, where n is the number of source nodes in a network, which can be obtained by using the nearest-neighbor routing and the optimal capacity scaling of a random static network was shown to be $\Theta(\sqrt{n/\log n})$ which can be obtained by acting nodes in a time division multiple access (TDMA) manner to reduce interference from other transmitters. Also, after that seminal work, the capacity scaling of various network models and assumptions have been proposed and the optimum media access control (MAC) protocols for achieving the capacity scaling

have been developed [2]–[9]. In [10][11], the capacity scaling of a random static network with practical MAC protocols was analyzed. In [10], a slotted ALOHA protocol for multi-hop transmission is considered and it was shown that the capacity scaling is greater than or equal to $\Theta(1)$ if the media access probability of each node is optimized. In [11], it was shown that the optimal capacity scaling of an arbitrary network, $\Theta(\sqrt{n})$, can be achieved in a random static network with the aid of pure relays just by optimizing the number of hops of each end-to-end (e2e) link because a sufficiently large number of pure relays can make a random network into an arbitrary network.

Many services require packet delivery under a delay constraint, which here denotes the maximum allowed delay D for e2e packet delivery while satisfying some target outage probability ϵ . Also, it was seen in literature that the capacity scaling is affected by a delay constraint. In [12][13], the optimal scaling of a random static network is obtained as $\Theta(1)$ (i.e. the scaling exponent is zero) for a given constant delay constraint. However, simple MAC schemes used in [10][11] cannot provide the optimal scaling of $\Theta(1)$ in a delay-constrained wireless ad hoc network even if a sufficiently large number of pure relays help the packet delivery between source-destination pairs because of the constant delay constraint. Then, the following questions arise: is it possible to achieve the optimal scaling by using a MAC scheme based on a simple random access? If so, what will be the required additional features? Although the throughput-delay tradeoff was studied in [15][16], the above issues are not clearly answered yet.

In this paper, we consider a delay-constrained wireless ad hoc network using a MAC protocol based on the slotted ALOHA (SA) protocol. The additional features considered in this paper are multi-hop control (M), rate control (R), admission control (A), and interference control (I). Those control schemes can be used individually or together. For example, the SA with multi-hop control (SA-M) protocol controls the number of hops on each e2e link. The SA with multi-hop and rate control (SA-MR) protocol controls the number of hops and the transmission rate on each e2e link. The SA with multi-hop, rate, and interference control (SA-MRI) protocol controls the number of hops and the transmission rate of each e2e link and the e2e access probability of the whole network. The SA with multi-hop, admission, interference control (SA-MAI) protocol performs an admission control for each e2e link as well as controlling the number of hops and the e2e

Manuscript received March 13, 2012; revised July 21, 2012; accepted December 24, 2012. The associate editor coordinating the review of this paper and approving it for publication was S. Liew.

This work was supported by the National Research Foundation (NRF) of Korea grant funded by the Ministry of Education, Science and Technology (No. 2011-0029321).

I. Byun and K. S. Kim (corresponding author) are with the Department of Electronic and Electrical Engineering, Yonsei University, 50 Yonsei-ro, Seodaemun-gu, Seoul 120-749, Korea (e-mail:ks.kim@yonsei.ac.kr).

J. G. Andrews is with the Department of Electrical and Computer Engineering, UT Austin, 1 University Station, C0803, Austin, TX 78712.

Digital Object Identifier 10.1109/TWC.2013.013013.120358

media access probability¹. The performance metric considered in this paper is the *delay-constrained random access transport capacity* (D-RATC), which characterizes the maximum average e2e rate per unit area that can be reliably delivered to the destination from the source within the maximum allowed delay D with success probability at least $1 - \epsilon$. The main contributions of this paper can be summarized as follows.

- 1) In a delay-constrained wireless multi-hop networks, the D-RATC scaling of the SA-M, SA-I, SA-A, SA-MI, or SA-MA protocol is $\Theta(0)$ (i.e., the scaling exponent is negative infinity), the D-RATC scaling of the SA-R or SA-MR protocol is $\Theta(\lambda_e^{-\alpha/2+1})$, where λ_e is the average number of source nodes per unit area and $\alpha > 2$ is the path-loss exponent, and the D-RATC scaling of the SA-RI, SA-AI, SA-MRI, or SA-MAI protocol is $\Theta(1)$.
- 2) The optimal scaling cannot be achieved without interference control. In addition, interference control needs an additional feature such as rate or admission control. Multi-hop control just improves the pre-constant but not the scaling exponent of the D-RATC.

The remainder of this paper is organized as follows. In Section II, the network model and MAC protocols are introduced. In Section III, the D-RATC and the scaling exponent of the D-RATC are derived. In Section IV, the D-RATC scalings of various MAC protocols based on the SA protocol and the effect of each additional feature is described. In Section V, numerical results on the D-RATC scaling and the optimal values of controllable parameters are shown. Finally, concluding remarks are given in Section VI.

II. SYSTEM MODEL

We consider a large wireless network where the locations of nodes follow a homogeneous Poisson point process (PPP) Φ_n of density λ_n . In the network, a node could be a source with probability ρ_s , each source randomly selects its destination among nodes except the sources, and a source-destination pair selects its relays among nodes except the sources and destinations. In this paper, we call a source-destination pair with its relays as an *e2e link* and each hop in the e2e link as a constituent *point-to-point (p2p) link* as shown in Figure 1. Let \mathcal{E} be the index set of the e2e links in the network, $\mathcal{P}_i = \{1, 2, \dots, N_i\}$ be the index set of the p2p links in the i -th e2e link, where N_i is the number of hops in the i -th e2e link, and $x_{i,j} \in \Phi_n$ and $x_{i,j+1} \in \Phi_n$, $i \in \mathcal{E}$ and $j \in \mathcal{P}_i$, respectively be the locations of the transmitter and the receiver of the j -th p2p link in the i -th e2e link. Then, the i -th e2e link can also be represented by the locations of its constituent nodes as $\eta_i = (x_{i,1}, x_{i,2}, \dots, x_{i,N_i+1})$ and the j -th p2p link in the i -th e2e link can be similarly represented as $\varsigma_{i,j} = (x_{i,j}, x_{i,j+1})$, as summarized in Figure 1. Let $d_{xy} = |x - y|$. Then, the hop distance vector of the i -th e2e link is defined as $\mathbf{d}_i = (d_{i,1}, d_{i,2}, \dots, d_{i,N_i})$, where $d_{i,j} = d_{x_{i,j}, x_{i,j+1}}$ and $d_i = d_{x_{i,1}, x_{i,N_i+1}}$.

Let P be the transmit power at all transmitters and r_i (b/s/Hz) be the transmission rate of a packet in bit per channel

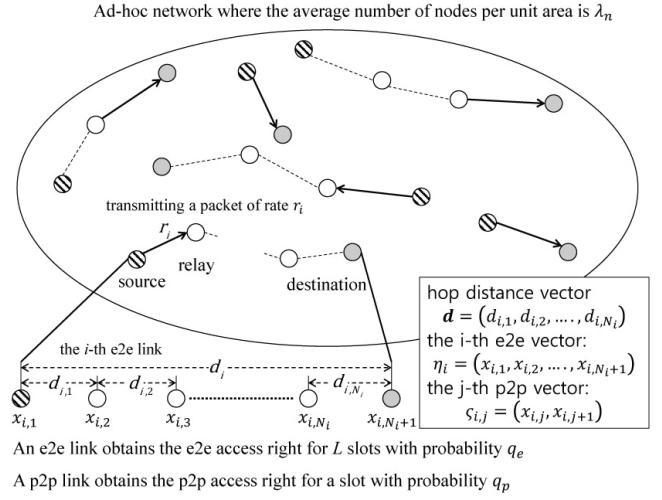


Fig. 1. Multi-hop ad hoc network model with the slotted ALOHA protocol having the e2e access probability q_e and p2p access probability q_p .

use of the i -th e2e link. In each e2e link, a packet transmitted at the source should be delivered to the destination within D slots with success probability of at least $1 - \epsilon$, where $0 < \epsilon < 1$ is independent of λ_e . Each source is assumed to have packets to send all the time and does not transmit the next packet until the previous transmitted packet is delivered to the destination or the number of slots elapsed for the packet reaches D^2 . The slotted ALOHA protocol considered in this paper can control the access of each e2e link similar to the MAC protocols in [18][19], or the access of each p2p link as in [20][21]. An e2e link obtains the e2e access right for L slots with the e2e media access probability q_e and can transmit packets until it expires³. If an e2e link fails to obtain e2e access rights, it attempts again after L slots. Once packet delivery begins, each p2p link has p2p access at a slot with probability q_p , if it has a packet to deliver. The packet travels to the destination using a hop-by-hop decode-and-forward principle with automatic repeat request (ARQ).

Let $\mathcal{E}_t \subset \mathcal{E}$ be the index set of the e2e links having the e2e access right at slot t and $\mathcal{P}_{i,t} \subset \mathcal{P}_i$ be the index set of the p2p links having the p2p access right at slot t . Then, the set of the locations of the transmitters at slot t is given by $\Phi_t = \{x_{i,j} \mid i \in \mathcal{E}_t, j \in \mathcal{P}_{i,t}\} \subset \Phi_n$ and follows a homogeneous PPP of density $\lambda = q_e q_p \lambda_e$, where $\lambda_e = \rho_s \lambda_n$ is the source density [17]. Let $d_{xy}^{-\alpha}$ and $h_{xy}[t] \sim \text{Exp}(1)$ be respectively the large-scale and the small-scale fading between nodes x and y . Then, the received SINR at the receiver $x_{i,j+1}$ of the j -th p2p link of the i -th e2e link in slot t , $\gamma_{i,j}[t]$, is given by

$$\gamma_{i,j}[t] = \frac{P d_{i,j}^{-\alpha} h_{x_{i,j}, x_{i,j+1}}[t]}{P \sum_{z \in \Phi_t \setminus \{x_{i,j}\}} d_{z, x_{i,j+1}}^{-\alpha} h_{z, x_{i,j+1}}[t] + N_0}, \quad (1)$$

where $N_0/2$ is the two-sided power spectral density of the additive white Gaussian noise (AWGN). Then, the comple-

²We assume appropriate ACK/NACK signalings among the transmitters and receivers in an e2e link. Note that the overhead for the ACK/NACK signaling is ignored because it does not affect the capacity scaling [12][13].

³The performance degradation due to the case where the number of remaining slots is less than D can be ignored by assuming $L \gg D$.

¹Note that, although the control schemes are very simplified and cannot cover all control schemes, they would be sufficient to show most of the impacts of an additional control scheme on the capacity scaling of wireless networks.

mentary cumulative distribution function (ccdf) of $\gamma_{i,j}[t]$ is given by

$$\begin{aligned} & \Pr\{\gamma_{i,j}[t] > 2^{r_i} - 1\} \\ & \triangleq p(d_{i,j}, r_i, q_e) \\ & = \exp\left(-\frac{2^{r_i} - 1}{d_{i,j}^{-\alpha} P/N_0} - q_e q_p \lambda_e (2^{r_i} - 1)^{\frac{2}{\alpha}} K_\alpha d_{i,j}^2\right), \end{aligned} \quad (2)$$

where $K_\alpha = 2\pi^2/(\alpha \sin(2\pi/\alpha)) [10]^4$. On each hop, a packet is transmitted with probability q_p and successfully decoded at the receiver with probability $p(d_{i,j}, r_i, q_e)$ if a packet is transmitted. Thus, the number of slots required for the successful transmission in the j -th p2p link of the i -th e2e link, $T_j(d_{i,j}, r_i, q_e)$, is a geometric random variable with success probability of $q_p p(d_{i,j}, r_i, q_e)$ and the total number of slots required for the successful transmission of a packet in the i -th e2e link, $T(\mathbf{d}_i, r_i, q_e)$, is given by

$$T(\mathbf{d}_i, r_i, q_e) = \sum_{j=1}^{N_i} T_j(d_{i,j}, r_i, q_e). \quad (3)$$

Also, the number of slots elapsed for packet delivery is given by $\min(T(\mathbf{d}_i, r_i, q_e), D)$. Then, similarly as in [24], the e2e outage probability and the throughput of the i -th e2e link can be respectively given by

$$P_{\text{out}}(D|\mathbf{d}_i, r_i, q_e) = \Pr\{T(\mathbf{d}_i, r_i, q_e) > D\} \quad (4)$$

and

$$R_\epsilon(D|\mathbf{d}_i, r_i, q_e) = r_i \frac{1 - \Pr\{T(\mathbf{d}_i, r_i, q_e) > D\}}{E[\min(T(\mathbf{d}_i, r_i, q_e), D)]} \quad (b/s/Hz). \quad (5)$$

Note that the outage probability (4) or the throughput (5) in a wireless ad hoc network is highly dependent on its communication protocol and most typical control mechanisms used for wireless ad hoc networks in literature, including [20][22][23], can be classified into a choice of transmission range (admission control), a transmission rate (rate control), the route from a source to its destination (multi-hop control), and a scheme to schedule the transmission of each node (interference control). In this paper, it is assumed that multi-hop control enables an e2e link to control the vector \mathbf{d}_i , admission control enables each source to choose the destination among nodes within a predetermined source-destination distance, rate control enables controlling r_i , and interference control enables controlling q_e . Also, it is assumed that a protocol selectively uses either rate control or admission control since the distance weighted throughput can be optimized by either adjusting the transmission rate for a given e2e distance or the e2e distance for a given transmission rate.

Let ψ be a random network using the SA- ψ protocol under the above assumptions, where $\psi \in \{M, R, I, A, MR, MI, MA, RI, AI, MRI, MAI\}$. Also, let $\Psi_M = \{M, MR, MI, MA, MRI, MAI\}$ be the protocol set using multi-hop control, $\Psi_A = \{A, MA, AI, MAI\}$ be the protocol set using admission control, $\Psi_R = \{R, MR, RI, MRI\}$ be the protocol set using rate

control, $\Psi_I = \{I, MI, RI, AI, MRI, MAI\}$ be the protocol set using interference control. Then, the set of all controllable parameter vectors of the i -th e2e link satisfying the delay constraint in network ψ is given by

$$\mathbf{U}_\epsilon^\psi(D|\mathbf{d}_i) = \{(\mathbf{d}_i, r_i, q_e) \in \mathcal{D}^\psi(d_i) \times \mathcal{R}^\psi \times \mathcal{Q}^\psi \mid \Pr\{T(\mathbf{d}_i, r_i, q_e) > D\} \leq \epsilon\}, \quad (6)$$

where $\mathcal{D}^\psi(d_i) = \mathcal{M}^\psi(d_i) \cap \mathcal{A}^\psi(d_i)$,

$$\mathcal{M}^\psi(d_i) = \begin{cases} \bigcup_{N_i=1}^D \{(d_{i,1}, d_{i,2}, \dots, d_{i,N_i}) \\ |d_{i,j} \in (0, \infty), \sum_{j=1}^{N_i} d_{i,j} \geq d_i\}, & \text{if } \psi \in \Psi_M, \\ \{\text{a given } (d_{i,1}, d_{i,2}, \dots, d_{i,N_i})\}, & \text{if } \psi \notin \Psi_M, \end{cases}$$

$$\mathcal{A}^\psi(d_i) = \begin{cases} \bigcup_{N_i=1}^D \{(d_{i,1}, d_{i,2}, \dots, d_{i,N_i}) \\ |d_{i,n} \in (0, \infty), \sum_{n=1}^{N_i} d_{i,n} \geq d_i\}, & (7) \\ \phi, & \text{if } \psi \in \Psi_A \text{ and } d_i \leq d_{i,\max} \text{ or } \psi \notin \Psi_A, \\ \phi, & \text{if } \psi \in \Psi_A \text{ and } d_i > d_{i,\max}, \end{cases}$$

$$\mathcal{R}^\psi = \begin{cases} (0, \infty), & \text{if } \psi \in \Psi_R, \\ \{\text{a given } r_i\}, & \text{if } \psi \notin \Psi_R, \end{cases} \quad (8)$$

and

$$\mathcal{Q}^\psi = \begin{cases} (0, 1], & \text{if } \psi \in \Psi_I, \\ \{\text{a given } q_e\}, & \text{if } \psi \notin \Psi_I. \end{cases} \quad (9)$$

Also, the average distance-weighted throughput of the network ψ , $R_\epsilon^\psi(D)$, when each e2e link uses $(\mathbf{d}_i, r_i, q_e) \in \mathbf{U}_\epsilon^\psi(D|\mathbf{d}_i)$ is given by

$$R_\epsilon^\psi(D) = \frac{1}{\nu} E_{\mathcal{E}} \left[\sum_{i \in \mathcal{E}} d_i R_\epsilon(D|\mathbf{d}_i, r_i, q_e) \right], \quad (10)$$

where ν denotes the network area and $E_{\mathcal{E}}[\cdot]$ denotes the expectation over \mathcal{E} . In Tables I and II, the notations used in this paper are summarized.

III. DELAY-CONSTRAINED RANDOM ACCESS TRANSPORT CAPACITY

In this paper, the D-RATC is used as the performance metric and the D-RATC scaling of a random static network is analyzed according to a given MAC protocol.

Definition 1: (D-RATC) The D-RATC of network ψ , $C_\epsilon^\psi(D)$, is the average end-to-end rate per channel use and per unit area of network ψ that can be reliably delivered within at most D time slots satisfying the target outage probability ϵ when $(\mathbf{d}_i, r_i, q_e) \in \mathbf{U}_\epsilon^\psi(D|\mathbf{d}_i)$ is optimized for each e2e link, $i \in \mathcal{E}$, which is given by

$$C_\epsilon^\psi(D) \triangleq \begin{cases} \frac{1}{\nu} E_{\mathcal{E}} \left[\sum_{i \in \mathcal{E}} d_i \max_{(\mathbf{d}_i, r_i, q_e) \in \mathbf{U}_\epsilon^\psi(D|\mathbf{d}_i)} \frac{r(1 - \Pr\{T(\mathbf{d}_i, r_i, q_e) > D\})}{E[\min(T(\mathbf{d}_i, r_i, q_e), D)]} \right], \\ \text{if } \mathbf{U}_\epsilon^\psi(D|\mathbf{d}_i) \neq \phi \forall i \in \mathcal{E}, \\ 0, \text{ otherwise.} \end{cases} \quad (11)$$

For better mathematical tractability, we consider a typical e2e link with distance of d and the destination located at

⁴If $\alpha = 2$, the equation (2) is not valid because the cumulated interference power goes to infinity because the interferers' signals do not decay fast enough to keep the cumulated interference power finite [28].

TABLE I
NOTATIONS FOR THE WHOLE NETWORK.

Notation	Definition/explanation
D	the maximum number of slots allowed for transmitting a packet
ϵ	the target outage probability
λ_n	the node density
$\lambda_e = \rho_s \lambda_n$	the source density
q_e	the e2e access probability
q_p	the p2p access probability
$\lambda = q_e q_p \lambda_e$	the average number of transmitting nodes per unit area
P	the transmit power
$R_e^\psi(D)$	the average distance-weighted throughput of network ψ
$C_e^\psi(D)$	the D-RATC of network ψ
$a_e^\psi(D)$	the scaling exponent of network ψ

TABLE II
NOTATIONS FOR AN E2E LINK.

Notation	Definition/explanation
$\gamma_{i,j}[t]$	the received SINR of the j -th p2p link of the i -th e2e link in slot t
$\mathbf{T}_j(d_{i,j}, r_i, q_e)$	the number of slots for delivering a packet at the j -th p2p link of the i -th e2e link
$\mathbf{T}(d_i, r_i, q_e)$	the number of slots for delivering a packet in the i -th e2e link
$P_{\text{out}}(D \mathbf{d}_i, r_i, q_e)$	the e2e outage probability of the i -th e2e link
$R_e(D \mathbf{d}_i, r_i, q_e)$	the e2e throughput of the i -th e2e link
$\mathbf{U}_e^\psi(D d_i)$	the set of all controllable parameter vectors satisfying the delay constraint of the i -th e2e link with the e2e distance of d_i
$C_e^\psi(D d)$	the transport capacity of a typical e2e link with distance d

the origin rather than the average over the whole network, similarly as in [11][14].

Definition 2: (typical D-RATC) The typical D-RATC, $C_e^\psi(D|d)$, is defined as the D-RATC of network ψ under the assumption that each source has its destination at a fixed distance d , given by

$$C_e^\psi(D|d) \triangleq \begin{cases} d \max_{(\mathbf{d}, r, q_e) \in \mathbf{U}_e^\psi(D|d)} q_e \lambda_e \frac{r(1 - \Pr\{T(\mathbf{d}, r, q_e) > D\})}{E[\min(T(\mathbf{d}, r, q_e), D)]}, & \text{if } \mathbf{U}_e^\psi(D|d) \neq \emptyset, \\ 0, & \text{if } \mathbf{U}_e^\psi(D|d) = \emptyset, \end{cases} \quad (12)$$

where $\mathbf{d} = (d_1, \dots, d_N)$ denotes the N -dimensional hop distance vector and r (b/s/Hz) is the transmission rate per channel use of the typical e2e link.

Remark: The proposed D-RATC can be considered as an extension of the transmission capacity in [14] to a multi-hop retransmission scenario in which a rout adaptation is allowed. If D goes to infinity, $\lim_{D \rightarrow \infty} C_e^M(D)$ is equal to the random access transport capacity for simple MAC schemes introduced in [11].

Definition 3: (D-RATC scaling exponent) The D-RATC scaling exponent of network ψ , $a_e^\psi(D)$, is defined as the order of growth of the D-RATC as λ_e increases, given by

$$a_e^\psi(D) \triangleq \begin{cases} \lim_{\lambda_e \rightarrow \infty} \frac{\log(C_e^\psi(D|d))}{\log(\lambda_e)}, & \text{if } C_e^\psi(D|d) > 0, \\ -\infty, & \text{if } C_e^\psi(D|d) = 0. \end{cases} \quad (13)$$

Remark: Although $a_e^\psi(D)$ is obtained from $C_e^\psi(D|d)$, it is equal to $\lim_{\lambda_e \rightarrow \infty} \log C_e^\psi(D) / \log \lambda_e$ since the D-RATC

scaling is independent to the value of d if $d \in (0, \infty)$ as shown in [11][14].

For easy analysis, we assume that $\lambda_n \gg \lambda_e \gg 1$, which denotes that the number of possible relay nodes is sufficiently large⁵. In this case, we can assume that the selected relays form a line between the source and the destination and the hop distance is equidistant, i.e. $\mathbf{d} = (d/N, \dots, d/N)$, where $|\mathbf{d}| = N$. Thus, $\mathcal{M}^\psi(d)$ can be simplified as $\bar{\mathcal{M}}^\psi(d) = \bigcup_{N=1}^D \{(d_1, d_2, \dots, d_N) \mid d_n = d/N, n = 1, \dots, N\}$, where $\bar{\mathcal{D}}^\psi(d) = \bar{\mathcal{M}}^\psi(d) \cap \mathcal{A}^\psi(d)$. By adopting the equidistance linear model, multi-hop control and admission control can be simplified so that multi-hop control optimizes the number of hops N only and admission control determines the allowed maximum transmission range d_{\max} of a possible e2e link. Here, note that d_{\max} should not be vanishing even though $\lambda_e \rightarrow \infty$. In the equidistance linear model, $T(\mathbf{d}, r, q_e)$ is given as the sum of N independent and identically distributed random variables $\sum_{i=1}^N T_j(d/N, r, q_e)$, where $T_j(d/N, r, q_e)$ is a geometric random variable with success probability $q_p p(D/N, r, q_e)$. Then, the e2e outage probability is given by

$$P_{\text{out}}(D|\mathbf{d}, r, q_e) = \Pr\{T(\mathbf{d}, r, q_e) > D\} \quad (14)$$

$$= \Pr\left\{\sum_{i=1}^N T_j(d/N, r, q_e) > D\right\} \quad (15)$$

$$= \sum_{k=0}^{N-1} \binom{D}{k} \left(q_p p\left(\frac{d}{N}, r, q_e\right)\right)^k \times \left(1 - q_p p\left(\frac{d}{N}, r, q_e\right)\right)^{D-k} \quad (16)$$

$$= 1 - \frac{B\left(q_p p\left(\frac{d}{N}, r, q_e\right); N, D - N + 1\right)}{B(N, D - N + 1)}, \quad (17)$$

where $B(a, b)$ is the beta function and $B(x; a, b)$ is the incomplete beta function [19]. Also, the set of controllable parameter vectors in (6) can be rewritten as

$$\mathbf{U}_e^\psi(D|d) = \left\{(\mathbf{d}, r, q_e) \in \bar{\mathcal{D}}^\psi(d) \times \mathcal{R}^\psi \times \mathcal{Q}^\psi \mid p\left(\frac{d}{N}, r, q_e\right) \geq \frac{p_e(D, N)}{q_p}\right\}, \quad (18)$$

where $p_e(D, N)$ denotes the minimum successful transmission probability per each hop required for the N -hop e2e link to satisfy the delay constraint, which can be obtained from (17) as

$$p_e(D, N) = B^{-1}\left((1 - \epsilon)B(N, D - N + 1); N, D - N + 1\right), \quad (19)$$

where $B^{-1}(y; a, b)$ is the inverse incomplete beta function [27]. Although $B^{-1}(y; a, b)$ is not given in a closed form, (19) can be easily evaluated for given ϵ , D , and N using a numerical method [27]. Also, note that if $q_p < p_e(D, N)$, $\mathbf{U}_e^\psi(D|d)$ becomes empty.

⁵Note that it will be shown at the end of Section IV that relaxing the assumption does not change the D-RATC scaling.

IV. THE D-RATC SCALING EXPONENT

The main result of this section is given in the following theorem.

Theorem 1. The D-RATC scaling exponent of network ψ is given by

$$\begin{aligned} a_\epsilon^M(D) &= a_\epsilon^I(D) = a_\epsilon^A(D) \\ &= a_\epsilon^{MI}(D) = a_\epsilon^{MA}(D) = -\infty, \end{aligned} \quad (20)$$

$$a_\epsilon^R(D) = a_\epsilon^{MR}(D) = -\frac{\alpha}{2} + 1, \quad (21)$$

$$a_\epsilon^{RI}(D) = a_\epsilon^{AI}(D) = a_\epsilon^{MRI}(D) = a_\epsilon^{MAI}(D) = 0. \quad (22)$$

Proof: It is straightforward that

$$\begin{aligned} d \max_{(\mathbf{d}, r, q_e) \in \mathbf{U}_\epsilon^\psi(D|d)} \frac{q_e \lambda_e r (1 - \epsilon)}{E[\min(T(\mathbf{d}, r, q_e), D)]} &\leq C_\epsilon^\psi(D|d) \\ &\leq d \max_{(\mathbf{d}, r, q_e) \in \mathbf{U}_\epsilon^\psi(D|d)} \frac{q_e \lambda_e r}{E[\min(T(\mathbf{d}, r, q_e), D)]} \end{aligned} \quad (23)$$

from (12) because $1 - \epsilon \leq 1 - \Pr\{T(\mathbf{d}, r, q_e) > D\} \leq 1$ for $(\mathbf{d}, r, q_e) \in \mathbf{U}_\epsilon^\psi(D|d)$. Since, $\lim_{\lambda_e \rightarrow \infty} \frac{\log E[\min(T(\mathbf{d}, r, q_e), D)]}{\log \lambda_e} = 0$ and $\lim_{\lambda_e \rightarrow \infty} \frac{\log(1 - \epsilon)}{\log \lambda_e} = 0$, the D-RATC scaling exponent can be obtained as

$$a_\epsilon^\psi(D) = \begin{cases} 1 + \tilde{a}_\epsilon^\psi(D), & \text{if } \mathbf{U}_\epsilon^\psi(D|d) \neq \emptyset, \\ -\infty, & \text{if } \mathbf{U}_\epsilon^\psi(D|d) = \emptyset, \end{cases} \quad (24)$$

where

$$\tilde{a}_\epsilon^\psi(D) = \lim_{\lambda_e \rightarrow \infty} \frac{\log \left(d \max_{(\mathbf{d}, r, q_e) \in \mathbf{U}_\epsilon^\psi(D|d)} q_e r \right)}{\log(\lambda_e)}. \quad (25)$$

Equation (25) is evaluated for the cases of SA-M, SA-R and SA-MR in Appendix A, SA-I, SA-MI, SA-RI, SA-MRI in Appendix B, and SA-A, SA-MA, SA-AI, and SA-MAI in Appendix C, respectively to obtain (20)-(22). ■

From (20), it is seen that a multi-hop control scheme (as in [11]) is not order-optimal in a delay-constrained network although it was order-optimal without a delay constraint. From (21), it is shown that a rate control scheme, regardless of optimizing the number of hops, can provide a finitely negative scaling exponent but not optimal without interference control. From (20), it is shown that an interference control scheme over network (as in [10]) is not order-optimal without an additional feature. However, as shown in (22), an interference control scheme combined with an additional feature can provide the order-optimal scaling exponent in a delay-constrained network. In [12], it was shown that the order optimal scaling is achieved when a Genie-aided time division multiple access (TDMA) protocol is used, which is unrealistic for ad hoc networks because a central controller is required to perform the protocol. In this work, however, it is shown that the order optimal scaling can be achieved by using a simple ALOHA-based protocol with an additional feature.

A. Effect of interference control on the scaling exponent

An interference control scheme can maintain the average SINR at each receiver and the density of transmitters at a snapshot by controlling q_e inversely proportional to λ_e . In a

network without any delay constraint, it was shown that an interference control scheme provides a finite scaling exponent [10]. However, in a delay-constrained network, negatively infinite scaling exponent is obtained by using interference control only because it cannot guarantee the packet delivery within the delay constraint for various e2e links with different distances. However, it provides the order-optimal scaling if combined with either rate control or admission control as shown in Theorem 1 because the delay constraint can be satisfied by controlling the rate of each e2e link according to its distance or setting the maximum transmission range according to the given transmission rate.

B. Effect of rate control on the scaling exponent

A rate control scheme can adjust the transmission rate of a packet according to the average SINR at each receiver to guarantee the packet delivery within the delay constraint. Without interference control, SINR at a receiver decreases as $\lambda_e^{-\alpha/2}$. Thus, the transmission rate r decreases as $\lambda_e^{-\alpha/2}$ because $\log_2(1 + \text{SINR}) \simeq \text{SINR}/\log(2)$ when $\text{SINR} \ll 1$, which implies that the scaling exponent is $-\alpha/2 + 1$ since the D-RATC is approximately given as $\lambda_e r$. Although a rate control scheme does not provide the order-optimality alone, it can do if combined with interference control as shown in Theorem 1.

C. Effect of admission control on the scaling exponent

An admission control scheme controls a non-vanishing maximum transmission range d_{\max} for a network to satisfy the delay constraint for a given transmission rate r . When λ_e increases without interference control, the interference power increases as $\lambda_e^{\alpha/2}$ so that admission control only with a non-vanishing d_{\max} fails to satisfy the delay constraint, which implies that the scaling exponent is $-\infty$. However, when it is combined with interference control, the order optimal scaling can be achieved.

D. Effect of multi-hop control on the scaling exponent

In a network without delay constraint, it was shown that a multi-hop control scheme achieves the order-optimality, in which the optimal number of hops is proportional to $\sqrt{\lambda_e}$ [11]. However, in a delay-constrained network, a multi-hop control scheme cannot achieve the order-optimal scaling as shown in Theorem 1 because the hop distance cannot be smaller than a certain value in order to satisfy the delay constraint and the received SINR falls as λ_e increases, which implies that the delay constraint cannot be satisfied and the D-RATC collapses. However, the numerical results in Section V will show that multi-hop control does help to improve the pre-constant of the D-RATC.

Remark: From the fact that multi-hop control does not affect the capacity scaling due to a finite delay constraint, relaxing the assumption $\lambda_n \gg \lambda_e \gg 1$ does not affect the D-RATC scaling, which will be confirmed by simulation in Section V. Also, it is shown that any improved transmit protocol using a spatial reuse, such as in [10], may improve the pre-constant but cannot improve the D-RATC scaling.

V. NUMERICAL AND SIMULATION RESULTS

The typical D-RATC in (12) can be rewritten as

$$C_e^\psi(D|d) = d\lambda_e \times \max_{(\mathbf{d}, r, q_e) \in \mathcal{U}_e^\psi(D|d)} \frac{q_e r (1 - \Pr\{T(\mathbf{d}, r, q_e) > D\})}{N + \sum_{t=N}^{D-1} \Pr\{T(\mathbf{d}, r, q_e) > t\}}. \quad (26)$$

If r or q_e is controllable, $\mathcal{U}_e^\psi(D|d)$ becomes an infinite set. In this case, a finite set $\tilde{\mathcal{U}}_e^\psi(D|d) \subset \mathcal{U}_e^\psi(D|d)$ is constructed with a given resolution to reduce computational complexity and obtain an approximated value of the D-RATC by searching the optimal value of (\mathbf{d}, r, q_e) over $\tilde{\mathcal{U}}_e^\psi(D|d)$. For example, $\tilde{\mathcal{U}}_e^{\text{MRI}}(D|d)$ of the SA-MRI protocol can be obtained as follows. The controllable parameters of the SA-MRI protocol are N , r , and q_e . Here, $N \in \{1, 2, \dots, D\}$, $q_e \in (0, 1]$, and $r \in (0, r_{\max}(N, q_e)]$, where $r_{\max}(N, q_e)$ denotes the maximum value of r satisfying the delay constraint with given parameters N and q_e . Since q_e or r is within a finite interval, the region of (r, q_e) for a given N is quantized with a given resolution to construct a finite set $\tilde{\mathcal{U}}_e^{\text{MRI}}(D|d)$.

Figure 2 shows the D-RATC of the SA-M, SA-R, SA-MR, SA-RI, SA-MRI protocols according to λ_e when $D = 10$, $\epsilon = 0.1$, $q_p = 0.8$, and the received SNR at the reference point of $d = 1(m)$ is $SNR = 20\text{dB}$. This figure shows that the D-RATCs of those protocols increase as λ_e increases when λ_e is small. However, as λ_e increases over a certain value, the D-RATC of the SA-M protocol collapses and the D-RATC of the SA-(M)R protocol decreases but the D-RATC of the SA-(M)RI protocol remains, as expected from Theorem 1. Here, the D-RATC of the SA-M protocol collapses because it becomes impossible to satisfy the delay constraint by adjusting N for all $(\mathbf{d}, r, q_e) \in \bar{\mathcal{D}}^\psi(d) \times \mathcal{R}^\psi \times \mathcal{Q}^\psi$ in the region where $\lambda_e > \left(\log(q_p/p_e(D, N)) - \frac{2^r - 1}{d_j^{-\alpha} P/N_0} \right) / \left(q_e q_p (2^r - 1)^{\frac{2}{\alpha}} K_\alpha d_j^2 \right) \simeq 1.4 (1/m^2)$ in this case. Also, it is seen that multi-hop control can improve the pre-constant but not the scaling exponent as was expected.

Figures 3-6 show the optimum values of the parameters of the SA-RI and SA-MRI protocols according to λ_e and the delay constraint parameters D and ϵ when $q_p = 0.8$ and $SNR = 20\text{dB}$. Figure 3 shows that the optimum value of q_e , $q_{e,\text{opt}}$, is unity until λ_e reaches a certain threshold and decreases inversely proportional to λ_e after passing the threshold. This is because, when λ_e is small, the gain by increasing the number of e2e links is greater than the loss caused from the increased interference but, as λ_e increases, the loss outweighs the gain so that we need to maintain the interference level. This figure also shows that a larger interference level is endurable if multi-hop control is used, D increases, and ϵ increases. Figures 4 and 5 respectively show the optimum value of r , r_{opt} , of the SA-RI and SA-MRI protocols according to λ_e , D and ϵ . By comparing Figure 3 with Figures 4 and 5, it is seen that r_{opt} decreases as λ_e increases while $q_{e,\text{opt}}$ is unity until λ_e reaches a certain threshold and then remains still while $q_{e,\text{opt}}$ decreases when λ_e increases over the threshold. In other words, if the delay constraint can be satisfied when $q_e = 1$, the D-RATC is

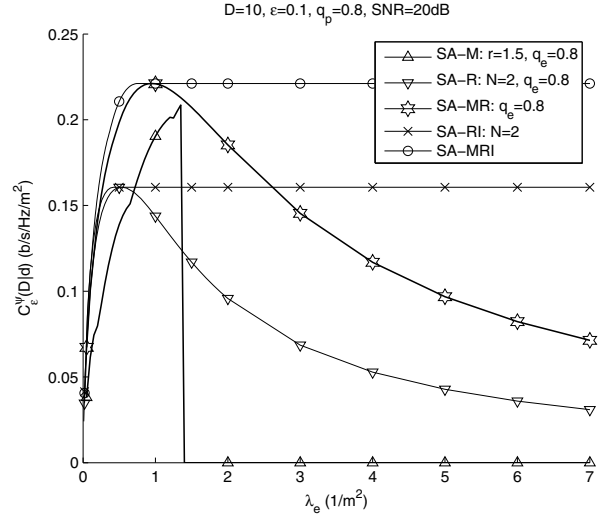


Fig. 2. D-RATC of the SA-M, SA-R, SA-MR, SA-RI, and SA-MRI protocols according to λ_e .

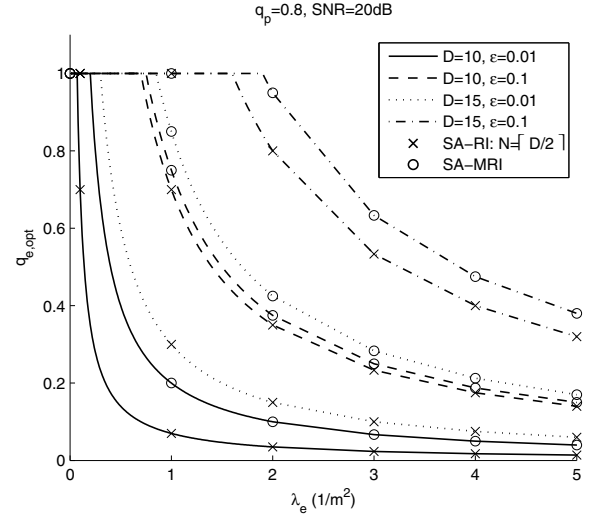


Fig. 3. The optimal e2e access probability $q_{e,\text{opt}}$ of the SA-RI and SA-MRI protocols for various delay constraint parameters.

maximized when $q_e = 1$. Unlike the SA-RI protocol case in Figure 5, the optimal rate in the SA-MRI protocol shows a jagged shape because the optimal number of hops, N_{opt} , changes discretely. As shown in Figure 6, N_{opt} increases as λ_e increases but should be kept much smaller than D for typical values of ϵ in order for the e2e outage probability not to be severely degraded due to the reduction of the allowed number of transmissions for a packet at each hop.

For the SA- φ protocol, $\varphi \in \{\text{AI}, \text{MAI}\}$, we consider a network where the allowed transmission coverage is at least d_{\min} and the controllable parameters and d_{\min} are arbitrarily chosen among the values satisfying the delay constraint, i.e., $\mathcal{U}_e^\varphi(D|d_{\min}) \neq \emptyset$. Figures 7-9 show $q_{e,\text{opt}}$ and the optimal transmission range d_{opt} maximizing the D-RATC of the SA-AI and SA-MAI protocols when $d_{\min} = 1(m)$, $q_p = 0.8$, $SNR = 20\text{dB}$. Figure 7 shows that $q_{e,\text{opt}}$ is unity until λ_e reaches a certain threshold but decreases inversely proportional to λ_e after the threshold as in the SA-RI and MRI protocols.

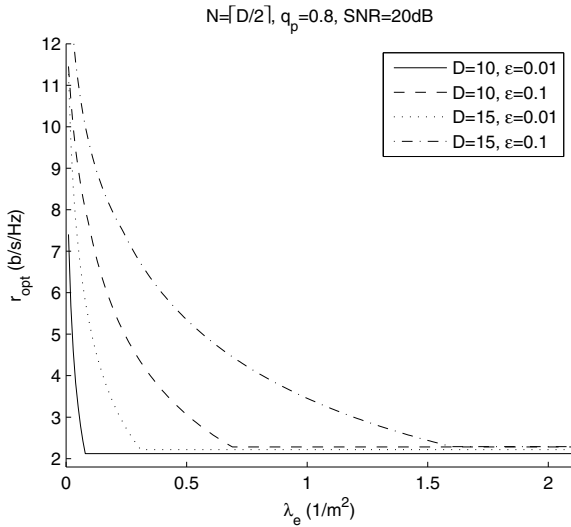


Fig. 4. The optimal rate r_{opt} of the SA-RI protocol for various delay constraint parameters.

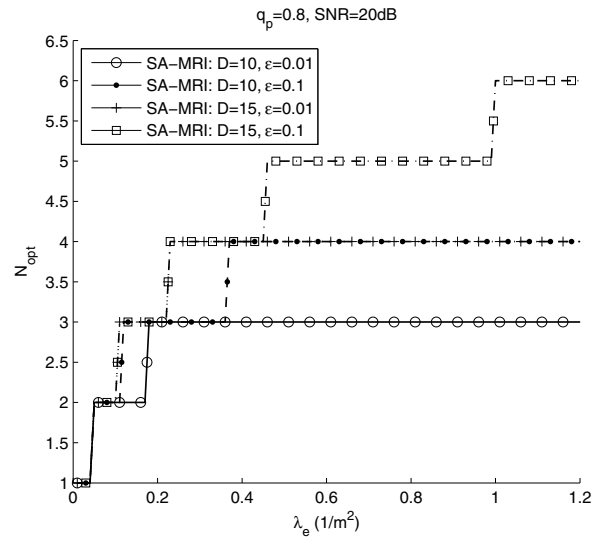


Fig. 6. The optimal number of hops N_{opt} of the SA-MRI protocol for various delay constraint parameters.

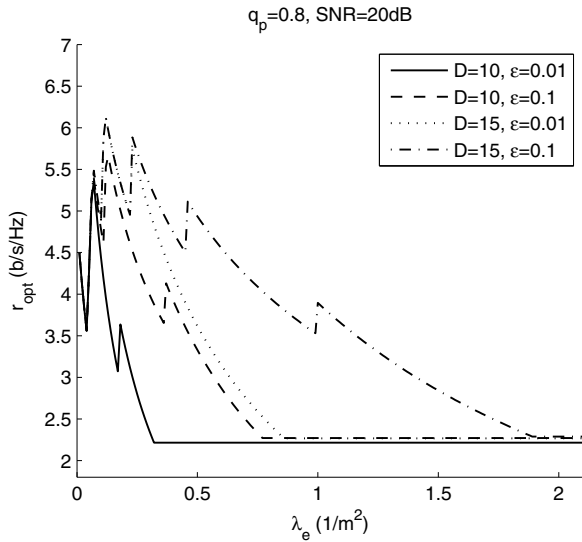


Fig. 5. The optimal rate r_{opt} of the SA-MRI protocol for various delay constraint parameters.

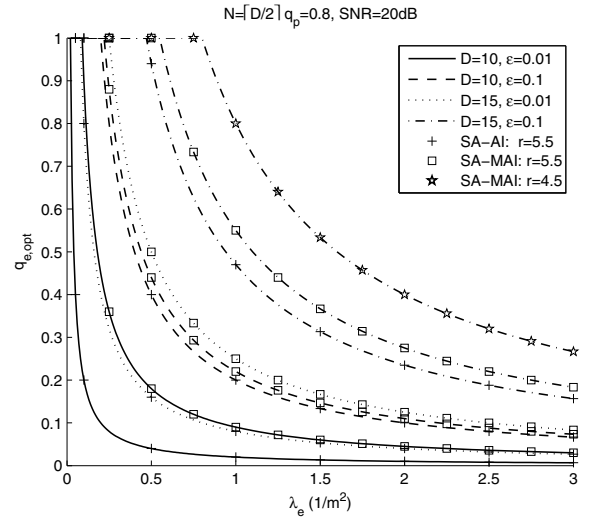


Fig. 7. The optimal e2e access probability $q_{e,opt}$ of the SA-AI and SA-MAI protocols for various delay constraint parameters.

Also, this figure shows that the threshold increases if multi-hop control is used, D increases, ϵ increases, and r decreases. Figure 8 shows that d_{opt} of the SA-AI protocol decreases and converges to d_{min} as λ_e increases. Also, the convergent point increases as D and ϵ increases. Figure 9 shows that d_{opt} tends to decrease as λ_e increases but d_{opt} of the SA-AI protocol shows a jagged shape because of the discrete characteristic of N_{opt} similarly as in r_{opt} of the SA-MRI protocol.

We obtain $R_e^\psi(D)$ of two practical parameter control schemes derived from Theorem 1, by simulation over a random static network. We assume that the receiver in a candidate p2p link estimates the average received SNR, \hat{E}_s , and the probabilities that the received SINR is greater than two arbitrarily chosen values β_1 and β_2 , respectively given by $\Pr\{\gamma > \beta_1\}$ and $\Pr\{\gamma > \beta_2\}$. Then, the receiver can estimate

the success probability as

$$G_\gamma(r; C(\alpha), q_e) = \exp\left(-\frac{2^r - 1}{\hat{E}_s} - q_e q_p C(\alpha) (2^r - 1)^{2/\alpha}\right) \quad (27)$$

from (2), where $C(\alpha) = \lambda_e K_\alpha d^2$. Here, $C(\alpha)$ and α can be estimated from the following two equalities given by

$$\Pr\{\gamma > \beta_k\} = \exp\left(-\frac{\beta_k}{\hat{E}_s} - q_e q_p C(\alpha) \beta_k^{2/\alpha}\right), \quad k = 1, 2. \quad (28)$$

After the route between a source and its destination is determined, each receiver in the route informs the estimated success probability $G_\gamma(r; C(\alpha), q_e)$ to its source.

The two practical parameter control schemes considered in this paper are respectively called the pSA-MRI scheme and the pSA-MAI scheme. The pSA-MRI scheme uses the destination-sequenced distance vector (DSDV) routing with the expected

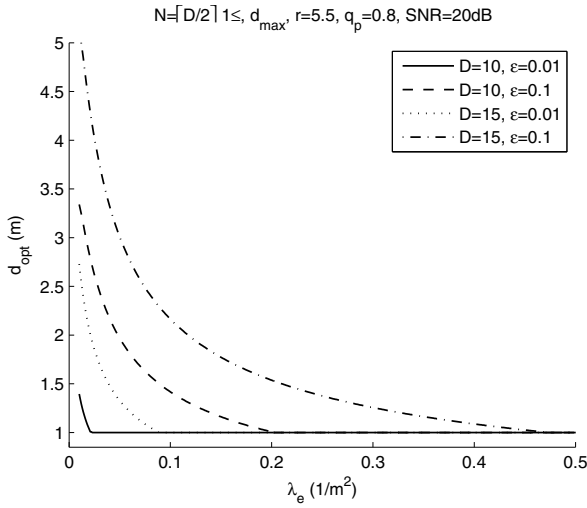


Fig. 8. The optimal e2e distance d_{opt} of the SA-AI protocols for various delay constraint parameters.

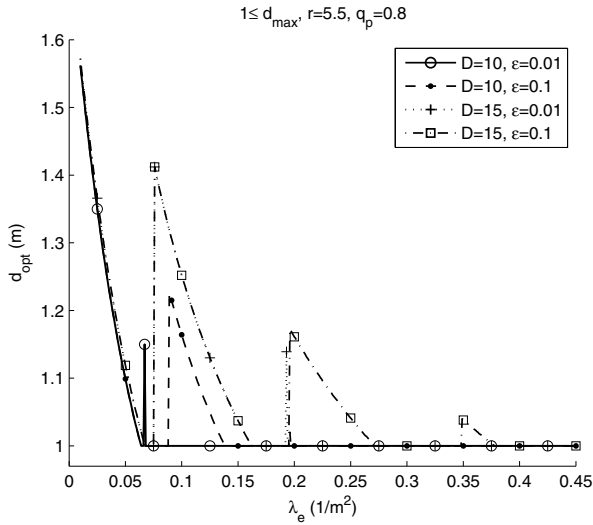


Fig. 9. The optimal e2e distance d_{opt} of the SA-MAI protocols for various delay constraint parameters.

slot count metric, $1/q_p p$, as the hop control [25]. The e2e access probability q_e of the pSA-MRI scheme is determined as $\min(1, A\lambda_e^{-1})$, where $A > 0$ is arbitrarily chosen. The initial transmission rate of the i -th e2e link is controlled as the maximum value of r satisfying the delay constraint as

$$r_i = G_\gamma^{-1} \left(\frac{p_\epsilon(D, N_i)}{q_p}; \max_{1 \leq j \leq N_i} C_{i,j}(\alpha), \min(1, A/\lambda_e^{-1}) \right), \quad (29)$$

where $C_{i,j}(\alpha) = \lambda_e K_\alpha d_{i,j}^2$. Here, $G_\gamma^{-1}(y; C(\alpha), q_e)$ can be easily obtained by using a bisection search algorithm since it is straightforward that $y = G_\gamma(r; C(\alpha), q_e)$ is a monotonically decreasing function of r . The pSA-MAI scheme also uses the same DSDV routing with the expected slot count metric and q_e is again determined as $\min(1, A\lambda_e^{-1})$ for arbitrarily chosen $A > 0$. If a selected e2e link using the DSDV algorithm cannot satisfy the delay constraint, the source randomly reselects its destination among nodes in the forward table of the DSDV algorithm except the previous destination until the delay constraint is satisfied. If the source cannot find its destination

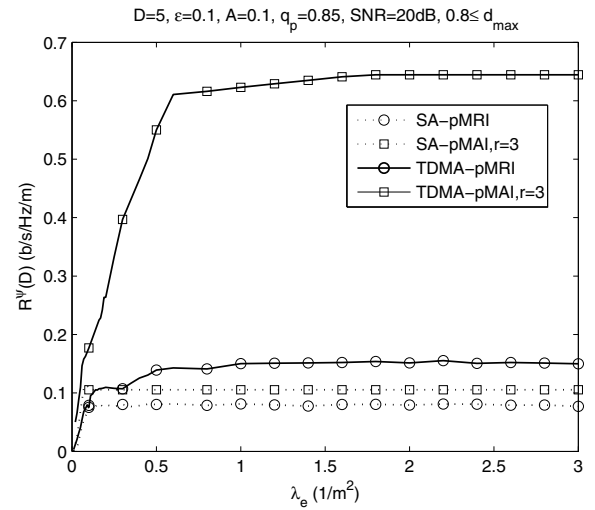


Fig. 10. $R^\psi(D)$ according to λ_e over a circular network with radius of $5(m)$.

satisfying the delay constraint among the forward table, the source is eliminated in the network.

For simulation, we consider a finite-size network where the locations of nodes follow a homogeneous PPP. Also, the pathloss exponent α is set to 4 and the minimum received signal power at the network edge is set to -38dB when the network radius is $5(m)$ and the transmitter is located at the origin. The average throughput $R_e^\psi(D)$ is obtained for the SA-pMRI, the SA-pMAI, the TDMA-pMRI, and the TDMA-pMAI protocols, where the TDMA-pMRI and the TDMA-pMAI protocols are Genie-aided TDMA MAC protocols similar to that in [12]. In those Genie-aided TDMA-based protocols, several distant nodes form a group and the nodes in the same group transmit signals simultaneously. The nodes in different groups are allocated in different time slots to reduce the interference power from other transmitters. Here, the group size yielding the best D-RATC is used for each value of λ_e among candidates.

Figure 10 shows $R_e^\psi(D)$ for $\varphi \in \{\text{pMRI}, \text{pMAI}, \text{TpMRI}, \text{TpMAI}\}$. This figure confirms that a simple practical scheme, such as the SA-pMRI or the SA-pMAI protocol, achieves the optimal capacity scaling although the typical D-RATC assumption and the equidistant hop assumption are relaxed. However, the pre-constant is significantly different from that of the Genie-aided TDMA protocol, which implies that it would be fruitful to devise a better interference control scheme to improve the D-RATC of a delay-constrained wireless ad hoc network.

VI. CONCLUSION

In this paper, a performance metric, called the *D-RATC*, which is a delay-constrained transport capacity with a random access MAC protocol is introduced and analyzed for random networks using simple SA-based MAC protocols. Most typical transmission control policies for wireless ad hoc networks are classified and simplified as multi-hop control, rate control, admission control, and interference control and then the D-RATC of a random network using a SA-based MAC protocol with

arbitrary combination of the above four additional features is analyzed in terms of the scaling exponent.

The analytic result reveals that the D-RATC is $\Theta(0)$ for the SA-M, SA-I, SA-A, SA-MI, or SA-MA protocol, $\Theta(\lambda_e^{-\alpha/2+1})$ for the SA-R or SA-RI protocol, and $\Theta(1)$ for the SA-RI, SA-AI, SA-MRI, or SA-MAI protocol, which implies that the optimal scaling of $\Theta(1)$ for a delay-constrained random network [12] can be achieved by using a simple SA-based MAC protocol when interference control is used with an additional feature such as rate control or admission control. Without an additional feature, it is shown that an SA-based MAC protocol with interference control only cannot achieve the optimal scaling because it does not guarantee the packet delivery within the delay constraint. Also, it is shown that, differently from the case without delay constraint shown in [11], multi-hop control improves the D-RATC pre-constant but cannot improve the D-RATC scaling.

It is also shown how the optimal values of the controllable parameters change according to the source density λ_e . When interference control is used with rate control (or admission control), the e2e access probability should be kept unity while decreasing transmission rate (or transmission coverage) as λ_e increases until λ_e reaches a certain threshold and then the e2e access probability should be decreased inversely proportional to λ_e without further change in the transmission rate (or transmission coverage). Also, simulation results confirmed that the optimal scaling can be achieved over a finite random static network even by using a simple and practical MAC protocol inspired from the SA-MRI or the SA-MAI.

APPENDIX A

From (2), as $\lambda_e \rightarrow \infty$, the SINR cdf of the SA-M protocol becomes

$$\begin{aligned} & \lim_{\lambda_e \rightarrow \infty} p\left(\frac{d}{N}, r, q_e\right) \\ &= \lim_{\lambda_e \rightarrow \infty} \exp\left(-\frac{2^r - 1}{\left(\frac{d}{N}\right)^{-\alpha} \frac{P}{N_0}} - q_e q_p \lambda_e (2^r - 1)^{\frac{2}{\alpha}} K_\alpha \left(\frac{d}{N}\right)^2\right) \\ &= 0 \end{aligned} \quad (30)$$

regardless of $N \leq D$ for any given constants r and q_e . Thus, $\lim_{\lambda_e \rightarrow \infty} \mathbf{U}_\epsilon^M(D|d) = \phi$, which implies $a_\epsilon^M(D) = -\infty$.

For the SA-protocol, the SINR cdf $p(d/N, r, q_e)$ is a monotonically decreasing function of r so that $\mathbf{U}_\epsilon^R(D|d)$ can be rewritten as

$$\begin{aligned} \mathbf{U}_\epsilon^R(D|d) &= \{(\mathbf{d}, r, q_e) \\ &| 0 < r \leq \log_2(1 + \beta(N, q_e)), \text{ given } \mathbf{d} \text{ and } q_e\}, \end{aligned} \quad (31)$$

where $\beta(N, q_e)$ is the value satisfying the equality $p(d/N, \log_2(1 + \beta(N, q_e)), q_e) = p_\epsilon(D, N)/q_p$. Let $x_1(N) = (d/N)^{-\alpha} P/N_0$ and $x_2(N) = q_p K_\alpha (d/N)^2$. Then, $\beta(N, q_e)$ can be upper and lower bounded as

$$\beta^{\text{lb}}(N, q_e) \leq \beta(N, q_e) \leq \min(\beta^{\text{ub}}(N, q_e), \beta_I^{\text{ub}}(N, q_e)), \quad (32)$$

where

$$\beta^{\text{ub}}(N, q_e) = \begin{cases} \frac{1}{x_1(N) + q_e \lambda_e x_2(N)} \log\left(\frac{q_p}{p_\epsilon(D, N)}\right), & \text{for } \beta(N, q_e) \in (0, 1), \\ \left(\frac{1}{x_1(N) + q_e \lambda_e x_2(N)} \log\left(\frac{q_p}{p_\epsilon(D, N)}\right)\right)^{\frac{\alpha}{2}}, & \text{for } \beta(N, q_e) \in [1, \infty), \end{cases} \quad (33)$$

$$\beta^{\text{lb}}(N, q_e) = \begin{cases} \left(\frac{1}{x_1(N) + q_e \lambda_e x_2(N)} \log\left(\frac{q_p}{p_\epsilon(D, N)}\right)\right)^{\frac{\alpha}{2}}, & \text{for } \beta(N, q_e) \in (0, 1), \\ \frac{1}{x_1(N) + q_e \lambda_e x_2(N)} \log\left(\frac{q_p}{p_\epsilon(D, N)}\right), & \text{for } \beta(N, q_e) \in [1, \infty), \end{cases} \quad (34)$$

and

$$\beta_I^{\text{ub}}(N, q_e) = \left(\frac{1}{\lambda_e q_e x_2(N)} \log\left(\frac{q_p}{p_\epsilon(D, N)}\right)\right)^{\frac{\alpha}{2}}, \quad (35)$$

because the upper and the lower bounds in (33) and (34) are respectively obtained from the facts that $\exp\left(-\left(x_1(N) + q_e \lambda_e x_2(N)\right) (2^r - 1)^{\frac{2}{\alpha}}\right) < p\left(\frac{d}{N}, r, q_e\right) < \exp\left(-\left(x_1(N) + q_e \lambda_e x_2(N)\right) (2^r - 1)\right)$ for $r \in (0, 1)$ and $\exp\left(-\left(x_1(N) + q_e \lambda_e x_2(N)\right) (2^r - 1)\right) \leq p\left(\frac{d}{N}, r, q_e\right) \leq \exp\left(-\left(x_1(N) + q_e \lambda_e x_2(N)\right) (2^r - 1)^{\frac{2}{\alpha}}\right)$ for $r \in [1, \infty)$ and the upper bound in (35) is obtained from an upper bound of $p(d/N, r, q_e)$, given by $p(d/N, r, q_e) < \exp\left(-\lambda_e q_e x_2(N) (2^r - 1)^{\frac{2}{\alpha}}\right)$. Note that the scaling exponent of $\beta(N, q_e)$ is also bounded as

$$\begin{aligned} \lim_{\lambda_e \rightarrow \infty} \frac{\log(\beta^{\text{lb}}(N, q_e))}{\log(\lambda_e)} &\leq \lim_{\lambda_e \rightarrow \infty} \frac{\log(\beta(N, q_e))}{\log(\lambda_e)} \\ &\leq \min\left(\lim_{\lambda_e \rightarrow \infty} \frac{\log(\beta^{\text{ub}}(N, q_e))}{\log(\lambda_e)}, \lim_{\lambda_e \rightarrow \infty} \frac{\log(\beta_I^{\text{ub}}(N, q_e))}{\log(\lambda_e)}\right), \end{aligned} \quad (36)$$

in which $\lim_{\lambda_e \rightarrow \infty} \frac{\log \beta^{\text{lb}}(N, q_e)}{\log \lambda_e} = -\frac{\alpha}{2}$, $\lim_{\lambda_e \rightarrow \infty} \frac{\log \beta^{\text{ub}}(N, q_e)}{\log \lambda_e} = -1$ for $\beta(N, q_e) \in (0, 1)$, and $\lim_{\lambda_e \rightarrow \infty} \frac{\log \beta_I^{\text{ub}}(N, q_e)}{\log(\lambda_e)} = -\frac{\alpha}{2}$. For $\lambda_e > \log(q_p/p_\epsilon(D, N))/(q_e x_2(N))$, $\beta(N, q_e) \in (0, 1)$ so that the scaling exponent of $\beta(N, q_e)$ is obtained as

$$\lim_{\lambda_e \rightarrow \infty} \frac{\log(\beta(N, q_e))}{\log(\lambda_e)} = -\frac{\alpha}{2}. \quad (37)$$

Then, $\tilde{a}_\epsilon^R(D)$ is obtained as

$$\begin{aligned} \tilde{a}_\epsilon^R(D) &= \lim_{\lambda_e \rightarrow \infty} \frac{\log(d \max_{(\mathbf{d}, r, q_e) \in \mathbf{U}_\epsilon^R(D|d)} q_e r)}{\log \lambda_e} \\ &= \lim_{\lambda_e \rightarrow \infty} \frac{\log(\max_{(\mathbf{d}, r, q_e) \in \mathbf{U}_\epsilon^R(D|d)} r)}{\log \lambda_e} \\ &= \lim_{\lambda_e \rightarrow \infty} \frac{\log(\log_2(1 + \beta(N, q_e)))}{\log \lambda_e} \\ &= \lim_{\lambda_e \rightarrow \infty} \frac{\log(\beta(N, q_e)/\log 2)}{\log \lambda_e} \\ &= -\frac{\alpha}{2}. \end{aligned} \quad (38)$$

Here, the second equality holds because d and q_e are constants, the third equality holds because $\log_2(1 + \beta(N, q_e))$ is the maximum value of r , the fourth equality holds because

$\log_2(1+x) = x/\log(2)$ as $x \rightarrow 0$, and the fifth equality holds from (37). Also, the set of controllable parameter vectors of the SA-MR protocol can be written as $\mathbf{U}_\epsilon^{\text{MR}}(D|d) = \bigcup_{N=1}^D \mathbf{U}_\epsilon^{\text{R}}(D|d)$. Then, $\tilde{a}_\epsilon^{\text{MR}}(D)$ is similarly obtained as

$$\begin{aligned}
 \tilde{a}_\epsilon^{\text{MR}}(D) &= \lim_{\lambda_\epsilon \rightarrow \infty} \frac{\log(d \max_{(\mathbf{d}, r, q_\epsilon) \in \mathbf{U}_\epsilon^{\text{MR}}(D|d)} q_\epsilon r)}{\log \lambda_\epsilon} \\
 &= \lim_{\lambda_\epsilon \rightarrow \infty} \frac{\log(\max_{1 \leq N \leq D} \log_2(1 + \beta(N, q_\epsilon)))}{\log \lambda_\epsilon} \\
 &= -\frac{\alpha}{2}.
 \end{aligned} \tag{39}$$

APPENDIX B

For the SA-I protocol, the SINR cdf $p(d/N, r, q_\epsilon)$ is a monotonically decreasing function of q_ϵ so that $\mathbf{U}_\epsilon^{\text{I}}(D|d)$ can be rewritten as

$$\mathbf{U}_\epsilon^{\text{I}}(D|d) = \{(\mathbf{d}, r, q_\epsilon) \mid 0 < q_\epsilon \leq \min(\hat{q}_\epsilon(N, r), 1), \text{ given } \mathbf{d} \text{ and } r\}, \tag{40}$$

where $\hat{q}_\epsilon(N, r)$ is the value satisfying the equality $p(\frac{d}{N}, r, \hat{q}_\epsilon(N, r)) = p_\epsilon(D, N)/q_p$, which is given by

$$\begin{aligned}
 \hat{q}_\epsilon(N, r) &= \frac{N^2}{\lambda_\epsilon q_p (2^r - 1)^{\frac{2}{\alpha}} K_\alpha d^2} \\
 &\quad \times \left(\log \frac{q_p}{p_\epsilon(D, N)} - d^\alpha \frac{2^r - 1}{N^\alpha P/N_0} \right), \tag{41}
 \end{aligned}$$

for $d < d_{\text{AWGN}}(N, r) \triangleq \left(\frac{N^\alpha P}{(2^r - 1) N_0} \log \frac{q_p}{p_\epsilon(D, N)} \right)^{1/\alpha}$. For $d \geq d_{\text{AWGN}}(N, r)$, $\hat{q}_\epsilon(N, r) \leq 0$, which implies $\mathbf{U}_\epsilon^{\text{I}}(D|d) = \phi$. Similarly for the SA-MI protocol, $\mathbf{U}_\epsilon^{\text{MI}}(D|d)$ can be rewritten as

$$\begin{aligned}
 \mathbf{U}_\epsilon^{\text{MI}}(D|d) &= \bigcup_{N=1}^D \{(\mathbf{d}, r, q_\epsilon) \\
 &\quad \mid d_n = \frac{d}{N}, 0 < q_\epsilon \leq \min(\hat{q}_\epsilon(N, r), 1), \text{ a given } r\}, \tag{42}
 \end{aligned}$$

which is not empty only when $d < \max_{N \in \{1, 2, \dots, D\}} d_{\text{AWGN}}(N, r)$. Without a control on the distance, the e2e distance of some e2e links can be greater than $d_{\text{AWGN}}(N, r)$ in the SA-I protocol and $\max_{N \in \{1, 2, \dots, D\}} d_{\text{AWGN}}(N, r)$ in the SA-MI protocol, which implies that $\mathbf{U}_\epsilon^{\text{I}}(D|d) = \phi$ and $\mathbf{U}_\epsilon^{\text{MI}}(D|d) = \phi$ (i.e., $a_\epsilon^{\text{I}}(D) = a_\epsilon^{\text{MI}}(D) = -\infty$) for some e2e links in a network.

For the SA-RI protocol, the delay constraint can be satisfied by controlling the transmission rate r for $q_\epsilon \in (0, 1]$ so that $\mathbf{U}_\epsilon^{\text{RI}}(D|d)$ can be rewritten as

$$\begin{aligned}
 \mathbf{U}_\epsilon^{\text{RI}}(D|d) &= \{(\mathbf{d}, r, q_\epsilon) \\
 &\quad \mid q_\epsilon \in (0, 1], 0 < r \leq \log_2(1 + \beta(N, q_\epsilon)), \text{ a given } \mathbf{d}\}. \tag{43}
 \end{aligned}$$

From (32) in Appendix A, we obtain

$$\begin{aligned}
 &\max_{q_\epsilon \in (0, 1]} q_\epsilon \log_2(1 + \beta(N, q_\epsilon)) \\
 &\leq \max_{q_\epsilon \in (0, 1]} \min(q_\epsilon \beta^{\text{ub}}(N, q_\epsilon), q_\epsilon \beta_I^{\text{ub}}(N, q_\epsilon)) \\
 &\leq \min \left(\max_{q_\epsilon \in (0, 1]} q_\epsilon \beta^{\text{ub}}(N, q_\epsilon), \max_{q_\epsilon \in (0, 1]} q_\epsilon \beta_I^{\text{ub}}(N, q_\epsilon) \right), \tag{44}
 \end{aligned}$$

where the first inequality holds since $\log_2(1+x) \leq x/\log 2$ for $x \in \mathbb{R}$ and the second inequality holds because $\max_{x \in \mathbb{R}} \min(f(x), g(x)) \leq \max_{x \in \mathbb{R}} f(x)$ and $\max_{x \in \mathbb{R}} \min(f(x), g(x)) \leq \max_{x \in \mathbb{R}} g(x)$. In (44), the optimal q_ϵ to maximize $q_\epsilon \beta^{\text{ub}}(N, q_\epsilon)$, q_ϵ^{ub} , is obtained as

$$q_\epsilon^{\text{ub}} = \begin{cases} 1, & \text{for } \beta(N, q_\epsilon) \in (0, 1), \\ \frac{x_1(N)}{\lambda_\epsilon x_2(N)^{(\alpha/2-1)}}, & \text{for } \beta(N, q_\epsilon) \in [1, \infty), \end{cases} \tag{45}$$

because, for $\beta(N, q_\epsilon) \in (0, 1)$,

$$\begin{aligned}
 &\frac{d(q_\epsilon \beta^{\text{ub}}(N, q_\epsilon))}{dq_\epsilon} \\
 &= \frac{d}{dq_\epsilon} \left(\frac{q_\epsilon}{x_1(N) + q_\epsilon \lambda_\epsilon x_2(N)} \log \left(\frac{q_p}{p_\epsilon(D, N)} \right) \right) \\
 &= \frac{1}{x_1(N) + q_\epsilon \lambda_\epsilon x_2(N)} \log \left(\frac{q_p}{p_\epsilon(D, N)} \right) \\
 &\quad - \frac{q_\epsilon \lambda_\epsilon x_2(N)}{(x_1(N) + q_\epsilon \lambda_\epsilon x_2(N))^2} \log \left(\frac{q_p}{p_\epsilon(D, N)} \right) \\
 &= \frac{x_1(N)}{(x_1(N) + q_\epsilon \lambda_\epsilon x_2(N))^2} \log \left(\frac{q_p}{p_\epsilon(D, N)} \right) \\
 &> 0
 \end{aligned} \tag{46}$$

and, for $\beta(N, q_\epsilon) \in [1, \infty)$,

$$\begin{aligned}
 &\frac{d(q_\epsilon \beta^{\text{ub}}(N, q_\epsilon))}{dq_\epsilon} \\
 &= \frac{d}{dq_\epsilon} \left[q_\epsilon \left(\frac{1}{x_1(N) + q_\epsilon \lambda_\epsilon x_2(N)} \log \left(\frac{q_p}{p_\epsilon(D, N)} \right) \right)^{\frac{\alpha}{2}} \right] \\
 &= \left(\frac{1}{x_1(N) + q_\epsilon \lambda_\epsilon x_2(N)} \log \left(\frac{q_p}{p_\epsilon(D, N)} \right) \right)^{\frac{\alpha}{2}} \\
 &\quad \times \left(1 - \frac{\alpha}{2} \frac{q_\epsilon \lambda_\epsilon x_2(N)}{x_1(N) + q_\epsilon \lambda_\epsilon x_2(N)} \right) \tag{47}
 \end{aligned}$$

becomes zero at $q_\epsilon = \frac{x_1(N)}{\lambda_\epsilon x_2(N)^{(\alpha/2-1)}}$. Thus, we obtain

$$\begin{aligned}
 &\max_{q_\epsilon \in (0, 1]} q_\epsilon \beta^{\text{ub}}(N, q_\epsilon) \\
 &= \begin{cases} \frac{1}{x_1(N) + q_\epsilon \lambda_\epsilon x_2(N)} \log \left(\frac{q_p}{p_\epsilon(D, N)} \right), & \text{for } \beta(N, q_\epsilon) \in (0, 1), \\ \left(\frac{\alpha}{2} - 1 \right)^{\alpha/2-1} \frac{\alpha - \alpha/2}{\lambda_\epsilon x_2(N) x_1(N)^{\alpha/2-1}} \left(\log \left(\frac{q_p}{p_\epsilon(D, N)} \right) \right)^{\alpha/2}, & \text{for } \beta(N, q_\epsilon) \in [1, \infty). \end{cases} \tag{48}
 \end{aligned}$$

Also, it is straightforward that

$$\sup_{q_\epsilon \in (0, 1]} q_\epsilon \beta_I^{\text{ub}}(N, q_\epsilon) = \infty, \tag{49}$$

since $q_\epsilon \beta_I^{\text{ub}}(N, q_\epsilon) \propto q_\epsilon^{1-\alpha/2}$. From (48) and (49), the scaling exponent of the upper bound in (44) is given as

$$\begin{aligned}
 &\lim_{\lambda_\epsilon \rightarrow \infty} \frac{\log \min \left(\max_{q_\epsilon \in (0, 1]} q_\epsilon \beta^{\text{ub}}(N, q_\epsilon), \max_{q_\epsilon \in (0, 1]} q_\epsilon \beta_I^{\text{ub}}(N, q_\epsilon) \right)}{\log \lambda_\epsilon} \\
 &= -1. \tag{50}
 \end{aligned}$$

From (32) in Appendix A, we obtain

$$\begin{aligned} & \max_{q_e \in (0,1]} q_e \log_2(1 + \beta(N, q_e)) \\ & \geq \max_{q_e \in (0,1]} q_e \log_2(1 + \beta^{\text{lb}}(N, q_e)) \\ & \geq A\lambda_e^{-1} \log_2(1 + \beta^{\text{lb}}(N, A\lambda_e^{-1})), \end{aligned} \quad (51)$$

where $A \in (0, \infty)$ and $\lambda_e \geq A$. If $q_e = A\lambda_e^{-1}$, then $\beta^{\text{lb}}(N, q_e)$ is given by

$$\beta^{\text{lb}}(N, A\lambda_e^{-1}) = \begin{cases} \left(\frac{1}{x_1(N) + Ax_2(N)} \log \left(\frac{q_p}{p_e(D, N)} \right) \right)^{\frac{\alpha}{2}}, & \text{for } \beta(N, A\lambda_e^{-1}) \in (0, 1), \\ \frac{1}{x_1(N) + Ax_2(N)} \log \left(\frac{q_p}{p_e(D, N)} \right), & \text{for } \beta(N, A\lambda_e^{-1}) \in [1, \infty), \end{cases} \quad (52)$$

which implies

$$\lim_{\lambda_e \rightarrow \infty} \frac{\log(A\lambda_e^{-1} \log_2(1 + \beta^{\text{lb}}(N, A\lambda_e^{-1})))}{\log \lambda_e} = -1. \quad (53)$$

Similarly as in Appendix A, $\tilde{a}_\epsilon^{\text{RI}}(D)$ and $\tilde{a}_\epsilon^{\text{MRI}}(D)$ can be respectively written as

$$\begin{aligned} & \tilde{a}_\epsilon^{\text{RI}}(D) \\ & = \lim_{\lambda_e \rightarrow \infty} \frac{\log(d \max_{(\mathbf{d}, r, q_e) \in \mathbf{U}_\epsilon^{\text{RI}}(D|d)} q_e r)}{\log \lambda_e} \\ & = \lim_{\lambda_e \rightarrow \infty} \frac{\log(\max_{(\mathbf{d}, r, q_e) \in \mathbf{U}_\epsilon^{\text{RI}}(D|d)} q_e r)}{\log \lambda_e} \\ & = \lim_{\lambda_e \rightarrow \infty} \frac{\log(\max_{q_e \in (0,1]} q_e \log_2(1 + \beta(N, q_e)))}{\log \lambda_e} \end{aligned} \quad (54)$$

and

$$\begin{aligned} & \tilde{a}_\epsilon^{\text{MRI}}(D) \\ & = \lim_{\lambda_e \rightarrow \infty} \frac{\log(d \max_{(\mathbf{d}, r, q_e) \in \mathbf{U}_\epsilon^{\text{MRI}}(D|d)} q_e r)}{\log \lambda_e} \\ & = \lim_{\lambda_e \rightarrow \infty} \frac{\log\left(\max_{1 \leq N \leq D} \max_{q_e \in (0,1]} q_e \log_2(1 + \beta(N, q_e))\right)}{\log \lambda_e}, \end{aligned} \quad (55)$$

where $\mathbf{U}_\epsilon^{\text{MRI}}(D|d) = \bigcup_{N=1}^D \mathbf{U}_\epsilon^{\text{RI}}(D|d)$. Then, from (50) and (53), we obtain $\tilde{a}_\epsilon^{\text{RI}}(D) = \tilde{a}_\epsilon^{\text{MRI}}(D) = -1$.

APPENDIX C

If admission control is used, the e2e distance d should be among $d \in (0, d_{\max}]$ so that $\tilde{a}_\epsilon^\varphi(D)$, $\varphi \in \{A, \text{MA}, \text{AI}, \text{MAI}\}$, can be redefined from (25) as

$$\tilde{a}_\epsilon^\varphi(D) = \begin{cases} \lim_{\lambda_e \rightarrow \infty} \frac{\log(d_{\max} \max_{(\mathbf{d}, r, q_e) \in \mathbf{U}_\epsilon^\varphi(D|d_{\max})} q_e r)}{\log(\lambda_e)}, & \text{if } d_{\max} > 0, \\ -\infty, & \text{if } d_{\max} = 0. \end{cases}$$

For the SA-A and the SA-MA protocols, upper bounds on d_{\max} to satisfy the delay constraint are respectively given by

$$d_{\max} \leq \sqrt{\frac{N^2}{q_e q_p \lambda_e (2^r - 1)^{2/\alpha} K_\alpha}} \log\left(\frac{q_p}{p_e(D, N)}\right) \quad (56)$$

and

$$\begin{aligned} d_{\max} & \leq \max_{N \in \{1, 2, \dots, D\}} N \sqrt{\log \frac{q_p}{p_e(D, N)}} \\ & \quad \times \frac{1}{\sqrt{q_e q_p \lambda_e (2^r - 1)^{2/\alpha} K_\alpha}} \end{aligned} \quad (57)$$

from the fact that $p(d/N, r, q_e) \leq \exp\left(-q_e q_p \lambda_e (2^r - 1)^{\frac{2}{\alpha}} K_\alpha d^2 N^{-2}\right)$. Thus, $\lim_{\lambda_e \rightarrow \infty} d_{\max} = 0$ for the SA-A and SA-MA protocols, which implies that $\tilde{a}_\epsilon^A(D) = \tilde{a}_\epsilon^{\text{MA}}(D) = -\infty$.

For the SA-AI protocol, if d is controlled as $d < d_{\text{AWGN}}(N, r)$, $\mathbf{U}_\epsilon^{\text{AI}}(D|d)$ can be rewritten as

$$\begin{aligned} & \mathbf{U}_\epsilon^{\text{AI}}(D|d) \\ & = \{(\mathbf{d}, r, q_e) \mid 0 < q_e \leq \min(\hat{q}_e(N, r), 1), \text{ given } \mathbf{d} \text{ and } r\} \\ & \neq \emptyset \end{aligned} \quad (58)$$

from (40). Since $d_{\text{AWGN}}(N, r)$ does not vanish as $\lambda_e \rightarrow \infty$, it is straightforward that d_{\max} also does not vanish as $\lambda_e \rightarrow \infty$. Then, similarly as in Appendix A, $\tilde{a}_\epsilon^{\text{AI}}(D)$ and $\tilde{a}_\epsilon^{\text{MAI}}(D)$ can be respectively written as

$$\begin{aligned} \tilde{a}_\epsilon^{\text{AI}}(D) & = \lim_{\lambda_e \rightarrow \infty} \frac{\log(d \max_{(\mathbf{d}, r, q_e) \in \mathbf{U}_\epsilon^{\text{AI}}(D|d)} q_e r)}{\log \lambda_e} \\ & = \lim_{\lambda_e \rightarrow \infty} \frac{\log(\max_{(\mathbf{d}, r, q_e) \in \mathbf{U}_\epsilon^{\text{AI}}(D|d)} q_e)}{\log \lambda_e} \\ & = \lim_{\lambda_e \rightarrow \infty} \frac{\log(\hat{q}_e(N, r))}{\log \lambda_e} \\ & = -1 \end{aligned} \quad (59)$$

and

$$\begin{aligned} \tilde{a}_\epsilon^{\text{MAI}}(D) & = \lim_{\lambda_e \rightarrow \infty} \frac{\log(d \max_{(\mathbf{d}, r, q_e) \in \mathbf{U}_\epsilon^{\text{MAI}}(D|d)} q_e r)}{\log \lambda_e} \\ & = \lim_{\lambda_e \rightarrow \infty} \frac{\log(\max_{N \in \{1, 2, \dots, D\}} \hat{q}_e(N, r))}{\log \lambda_e} \\ & = -1, \end{aligned} \quad (60)$$

where $\mathbf{U}_\epsilon^{\text{MAI}}(D|d) = \bigcup_{N=1}^D \mathbf{U}_\epsilon^{\text{AI}}(D|d)$, because

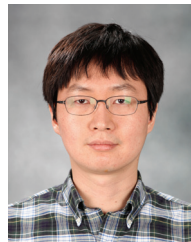
$$\lim_{\lambda_e \rightarrow \infty} \frac{\log(\hat{q}_e(N, r))}{\log(\lambda_e)} = -1 \quad (61)$$

from (41).

REFERENCES

- [1] P. Gupta and P. R. Kumar, "The capacity of wireless networks," *IEEE Trans. Inf. Theory*, vol. 46, no. 2, pp. 388–404, Mar. 2000.
- [2] M. Grossglauser and D. N. C. Tse, "Mobility increases the capacity of ad hoc wireless networks," *IEEE/ACM Trans. Networking*, vol. 10, no. 4, pp. 477–486, Aug. 2002.
- [3] M. Sikora, J. N. Laneman, M. Haenggi, D. J. Costello, and T. Fuja, "Bandwidth- and power-efficient routing in linear wireless networks," *IEEE Trans. Inf. Theory*, vol. 52, no. 6, pp. 2624–2633, June 2006.
- [4] A. Aeron and V. Saligrama, "Wireless ad hoc networks: strategies and scaling laws for the fixed SNR regime," *IEEE Trans. Inf. Theory*, vol. 53, no. 6, pp. 2044–2059, June 2007.
- [5] A. Özgür, O. Lévêque, and D. N. C. Tse, "Hierarchical cooperation achieves optimal capacity scaling in ad hoc networks," *IEEE Trans. Inf. Theory*, vol. 53, no. 10, pp. 3549–3572, Oct. 2007.
- [6] H. R. Sadjadpour, Z. Wang, and J. J. G.-L.-Aceves, "The capacity of wireless ad hoc networks with multi-packet reception," *IEEE Trans. Commun.*, vol. 58, no. 2, pp. 600–610, Feb. 2010.
- [7] L. Ying, S. Yang, and R. Srikant, "Optimal throughput-delay tradeoffs in mobile ad hoc networks," *IEEE Trans. Inf. Theory*, vol. 54, no. 9, pp. 4119–4143, Sep. 2008.

- [8] P. Li, Y. Fang, "Capacity and delay of hybrid wireless broadband access networks," *IEEE J. Sel. Areas Commun.*, vol. 27, no. 2, pp. 117–125, Feb. 2009.
- [9] A. Özgür and O. Lévêque, "Throughput-delay tradeoff for hierarchical cooperation in ad hoc wireless networks," *IEEE Trans. Inf. Theory*, vol. 56, no. 3, pp. 1369–1377, Mar. 2010.
- [10] F. Baccelli, B. Błaszczyszyn, and P. Mühlethaler, "An Aloha protocol for multihop mobile wireless networks," *IEEE Trans. Inf. Theory*, vol. 52, no. 2, Feb. 2006.
- [11] J. G. Andrews, S. Weber, M. Kountouris, and M. Haenggi, "Random access transport capacity," *IEEE Trans. Wireless Commun.*, vol. 9, no. 6, pp. 2101–2111, June 2010.
- [12] A. E. Gammal, J. Mammen, B. Prabhakar, and D. Shah, "Optimal throughput-delay scaling in wireless networks—part I: the fluid model," *IEEE Trans. Inf. Theory*, vol. 51, no. 6, pp. 2568–2592, June 2006.
- [13] A. E. Gammal, J. Mammen, B. Prabhakar, and D. Shah, "Optimal throughput-delay scaling in wireless networks—part II: constant-size packets," *IEEE Trans. Inf. Theory*, vol. 52, no. 11, pp. 5111–5116, Nov. 2006.
- [14] S. Weber, X. Yang, J. G. Andrews, and G. de Veciana, "Transmission capacity of wireless ad hoc networks with outage constraints," *IEEE Trans. Inf. Theory*, vol. 51, no. 12, pp. 4091–4102, Dec. 2005.
- [15] C. Comaniciu and H. V. Poor, "On the capacity of mobile ad hoc networks with delay constraints," *IEEE Trans. Wireless Commun.*, vol. 5, no. 8, pp. 2061–2071, Aug. 2006.
- [16] S. Srinivasa and M. Haenggi, "Throughput-delay-reliability tradeoff in multihop networks with random access," in *Proc. 2010 IEEE Annual Allerton Conf.*, pp. 1117–1124.
- [17] R. Vaze, "Throughput-delay-reliability tradeoff with ARQ in wireless ad hoc networks," *IEEE Trans. Wireless Commun.*, vol. 10, no. 7, pp. 2142–2149, July 2011.
- [18] P. Liu, Z. Tao, S. Narayanan, T. Korakis, and S. S. Panwar, "CoopMAC: a cooperative MAC for wireless LANs," *IEEE J. Sel. Areas Commun.*, vol. 25, no. 2, pp. 340–354, Feb. 2007.
- [19] C. Nie, P. Liu, T. Korakis, E. Erkip, and S. Panwar, "CoopMAX: a cooperative MAC with randomized distributed space-time coding for an IEEE 802.16 network," in *Proc. 2009 IEEE Conf. Int. Conf. on Commun.*, pp. 1–6.
- [20] B. G. Lee and S. Choi, *Broadband Wireless Access and Local Networks: Mobile WiMAX and WiFi*. Artech House, 2008.
- [21] Z. Hu and C. Tham, "CCMAC: coordinated cooperative MAC for wireless LANs," *Elsevier Computer Networks*, vol. 54, no. 4, pp. 618–630, Mar. 2010.
- [22] A. Wheeler, "Commercial applications of wireless sensor networks using Zigbee," *IEEE Commun. Mag.*, vol. 45, no. 4, pp. 70–77, Apr. 2007.
- [23] X. Shen, M. Guizani, R. C. Qiu, and T. Le-Ngoc, *Ultra-Wideband Wireless Communications and Networks*. John Wiley and Sons, Ltd., 2006.
- [24] G. Caire and D. Tuninetti, "The throughput of hybrid ARQ protocols for the Gaussian collision channel," *IEEE Trans. Inf. Theory*, vol. 47, no. 5, pp. 1971–1988, July 2001.
- [25] A. S. J. de Couto, D. Aguayo, J. Bicket, and R. Morris, "A high-throughput path metric for multi-hop wireless routing," *Springer Wireless Networks*, vol. 11, no. 4, pp. 419–434, July 2005.
- [26] E. S. Pearson and N. L. Johnson, *Tables of the Incomplete Beta-Function*, 2nd edition. Cambridge University Press, 1968.
- [27] D. W. Lozier and F. W. J. Olver, "Numerical evaluation of special functions," *Proc. Amer. Math. Soc. (AMS) Sympos. in Applied Mathematics*, vol. 48, no. 1, pp. 79–125, Dec. 1994.
- [28] M. Haenggi, J. G. Andrews, F. Baccelli, O. Dousse, M. Franceschetti, "Stochastic geometry and random graphs for the analysis and design of wireless networks," *IEEE J. Sel. Areas Commun.*, vol. 27, no. 7, pp. 1029–1046, Sep. 2009.



Ilmu Byun was born in Seongnam, Korea, on 28 May 1981. He received the B.S., M.S., and PhD degrees in electrical and electronic engineering from Yonsei University, Seoul, Korea in February 2005, February 2007, and February 2013, respectively. He is currently working with the LG electronics. His current research interests include rate-compatible channel codes, delay and energy constrained ad-hoc networks and hybrid networks.



Jeffrey G. Andrews (S'98, M'02, SM'06, F'13) received the B.S. in Engineering with High Distinction from Harvey Mudd College in 1995, and the M.S. and Ph.D. in Electrical Engineering from Stanford University in 1999 and 2002, respectively. He is a Professor in the Department of Electrical and Computer Engineering at the University of Texas at Austin, where he was the Director of the Wireless Networking and Communications Group (WNCG) from 2008–12. He developed Code Division Multiple Access systems at Qualcomm from 1995–97, and has

consulted for entities including the WiMAX Forum, Intel, Microsoft, Apple, Clearwire, Palm, Sprint, ADC, and NASA.

Dr. Andrews is co-author of two books, *Fundamentals of WiMAX* (Prentice-Hall, 2007) and *Fundamentals of LTE* (Prentice-Hall, 2010), and holds the Earl and Margaret Brasfield Endowed Fellowship in Engineering at UT Austin, where he received the ECE department's first annual High Gain award for excellence in research. He is a Senior Member of the IEEE, a Distinguished Lecturer for the IEEE Vehicular Technology Society, served as an associate editor for the IEEE TRANSACTIONS ON WIRELESS COMMUNICATIONS from 2004–08, was the Chair of the 2010 IEEE Communication Theory Workshop, and is the Technical Program co-Chair of ICC 2012 (Comm. Theory Symposium) and Globecom 2014. He is an elected member of the Board of Governors of the IEEE Information Theory Society and an IEEE Fellow.

Dr. Andrews received the National Science Foundation CAREER award in 2007 and has been co-author of five best paper award recipients, two at Globecom (2006 and 2009), Asilomar (2008), the 2010 IEEE Communications Society Best Tutorial Paper Award, and the 2011 Communications Society Heinrich Hertz Prize. His research interests are in communication theory, information theory, and stochastic geometry applied to wireless cellular and ad hoc networks.



Kwang Soon Kim (M'95, SM'04) was born in Seoul, Korea, on September 20, 1972. He received the B.S. (summa cum laude), M.S.E., and Ph.D. degrees in electrical engineering from Korea Advanced Institute of Science and Technology (KAIST), Daejeon, Korea, in February 1994, February 1996, and February 1999, respectively.

From March 1999 to March 2000, he was with the Department of Electrical and Computer Engineering, University of California at San Diego, La Jolla, CA, U.S.A., as a Postdoctoral Researcher. From April

2000 to February 2004, he was with the Mobile Telecommunication Research Laboratory, Electronics and Telecommunication Research Institute, Daejeon, Korea as a Senior Member of Research Staff. Since March 2004, he has been with the Department of Electrical and Electronic Engineering, Yonsei University, Seoul, Korea, now is an Associate Professor.

He was a recipient of the Postdoctoral Fellowship from Korea Science and Engineering Foundation (KOSEF) in 1999. He received the Outstanding Researcher Award from Electronics and Telecommunication Research Institute (ETRI) in 2002 and Jack Neubauer Memorial Award (Best system paper award, IEEE Transactions on Vehicular Technology) from IEEE Vehicular Technology Society in 2008. His research interests include communication theory, channel coding and iterative decoding, adaptive modulation and coding, cooperative communication, and wireless CDMA/OFDM systems.